CIRCADIAN RHYTHMS

Cell-autonomous clock of astrocytes drives circadian behavior in mammals

Marco Brancaccio*†, Mathew D. Edwards‡, Andrew P. Patton, Nicola J. Smyllie, Johanna E. Chesham, Elizabeth S. Maywood, Michael H. Hastings*

Circadian (~24-hour) rhythms depend on intracellular transcription-translation negative feedback loops (TTFLs). How these self-sustained cellular clocks achieve multicellular integration and thereby direct daily rhythms of behavior in animals is largely obscure. The suprachiasmatic nucleus (SCN) is the fulcrum of this pathway from gene to cell to circuit to behavior in mammals. We describe cell type–specific, functionally distinct TTFLs in neurons and astrocytes of the SCN and show that, in the absence of other cellular clocks, the cell-autonomous astrocytic TTFL alone can drive molecular oscillations in the SCN and circadian behavior in mice. Astrocytic clocks achieve this by reinstating clock gene expression and circadian function of SCN neurons via glutamatergic signals. Our results demonstrate that astrocytes can autonomously initiate and sustain complex mammalian behavior.

The transcription-translation negative feedback loop (TTFL) mechanisms responsible for intracellular circadian (~24-hour) timekeeping in animals are understood in molecular detail (*1*). The TTFL of mammals involves transcriptional activation by Clock/Bmal1 heterodimers, which drive daytime expression of *Period* (*Per*) and *Cryptochrome* (*Cry*) genes through E-box regulatory sequences. After dimerization and transport to the nucleus, Per-Cry complexes repress Clock-Bmal1 activity during circadian night, until progressive degradation of Per-Cry allows initiation of a new cycle. This self-sustaining cell-autonomous TTFL is universally active across mammalian tissues, so how cellular clocks interact to achieve multicellular integration and ultimately direct daily rhythms of behavior is a matter of considerable interest. The suprachiasmatic nucleus of the hypothalamus (SCN) is the fulcrum of this pathway from gene to cell to circuit to behavior. Its tightly coordinated multicellular oscillations can continue indefinitely to direct internal synchronization of cellular clocks across the body. The conventional view is that robust pacemaking relies on the intrinsic interneuronal connectivity of the SCN, albeit with principles still largely unknown (*2*). However, circadian timekeeping in the SCN is also influenced by a sophisticated interplay between its neurons and astrocytes (*3*). In common with other cell types, astrocytes have a TTFL that is assumed to be maintained by input from SCN neurons (*4*, *5*). In light of the intimacy of astrocyte-neuron interactions in the SCN, however, we wondered whether SCN astrocytes really are "slaves" to their neuronal partners, or whether the SCN pacemaker might instead be considered a bipartite cellular system in which astrocytes can also direct neuronal time-keeping and behavior.

To address this, we used adeno-associated virus vectors (AAVs) and genetics to characterize the distinctive properties of the TTFLs of SCN astrocytes and neurons. We assessed cell type–specific TTFL function with an AAV encoding a Cre recombinase–dependent reporter (*6*) in which firefly luciferase is driven by a minimal mouse Cry1 promoter (*Cry1*) containing E-boxes (Cry1-Flex-Luc; Flex represents Cre-dependent flip-excision) (*7*, *8*). Cotransduction of SCN slices with AAVs driving Cre by the glial fibrillary acidic protein (GFAP) or human synapsin 1 (Syn) promoters restricted Cry1-Flex-Luc expression to astrocytes or neurons, respectively (*3*) (Fig. 1, A to F). Bioluminescent recording revealed sustained circadian oscillations of *Cry1*-Luc in both SCN neurons and astrocytes. Although these oscillations had the same period and robustness, measured by the relative amplitude error (RAE), their waveforms differed (Fig. 1F), reminiscent of the distinctive waveforms of intracellular calcium rhythms observed in astrocytes and neurons (*3*). These SCN slices were also cotransduced with AAVs encoding the calcium reporter GCaMP3 driven by the Syn promoter (Syn-GCaMP3) to track circadian concentrations of neuronal intracellular calcium ($[Ca^{2+}]_i$). We used this reporter, which peaks during the mid-circadian day [circadian time 6.5 hours (CT6.5)] (*3*, *9*), to internally register the circadian phase of the detected *Cry1*-Luc expression in SCN astrocytes and neurons. This showed that the peak of expression of astrocytically restricted *Cry1*-Luc was phase-delayed by ~6.5 hours (~CT17) when compared with that of the neurons, which peaked at ~CT11 (Fig. 1, B, C, and F). Thus, neurons and astrocytes of the SCN exhibit cell type–specific functionally distinct Cry1-Luc reporter TTFLs characterized by different phases and waveforms.

To test the potential contribution of the astrocytic TTFL to SCN time-keeping, we used cell type–specific genetic complementation in SCN of mice lacking both *Cry* genes (Cry1/2-null mice) (*10*). In the absence of the Cry repressors, the endogenous TTFL does not function, so molecular circadian oscillations, monitored by the Per2::Luc reporter, are compromised (*11*) (Fig. 1G). Generalized (pan-cellular) expression of Cry1 can initiate circadian molecular rhythms in Cry-deficient SCN slices (*8*). Using Cre-dependent AAVs encoding a Cry1::EGFP (enhanced green fluorescent protein) fusion protein driven by the *Cry1* promoter (*Cry1*-Flex-Cry1::EGFP), we expressed Cry1 specifically in either neurons or astrocytes of Cry1/2-null SCN restricted by Syn-Cre or GFAP-Cre. As anticipated, expressing Cry1 in neurons was sufficient to initiate self-sustained circadian oscillations of Per2::Luc in the SCN. Expression of Cry1::EGFP solely in astrocytes was also effective, however, highlighting astrocytes as pacemakers within the SCN circuit (fig. S1 and Fig. 1, G and H). Nevertheless, there were appreciable differences in both the early and the late phases of Cry1 expression between the two cell type–specific manipulations. The effects on Per2::Luc oscillations of neuronally restricted Cry1::EGFP became apparent within ~2 days posttransduction (dpt), whereas astrocytically restricted Cry1 took appreciably longer (>7 dpt) to initiate rhythms. In the later stages (11 to 15 dpt), Cry1 maintained stable oscillations longer than 24 hours (appropriate to a Cry2-null background) (*10*) when expressed in either neurons or astrocytes, although astrocytically dependent rhythms had a significantly shorter period than neuronally driven rhythms (Fig. 1H). Thus, not only SCN neurons but also astrocytes can autonomously initiate and sustain stable oscillations of clock gene expression in the SCN, and their instructive, rather than simply permissive, role is evidenced by the observed period differences.

As shown by SCN transplantation between animals with contrasting genetically specified circadian periods (*12*, *13*), the defining property of the SCN as the master circadian pacemaker is its ability to initiate circadian patterns of behavior, imposing its intrinsic periodicity to the rest of the body. We therefore tested whether the cell-autonomous astrocytic TTFL could drive circadian locomotor activity rhythms in otherwise "clockless" adult mice and compared them to rhythms of mice with similarly restricted manipulations of the neuronal TTFL (Fig. 2). The SCN of Cry1/2-null mice were stereotaxically injected with Cre-conditional AAV-*Cry1*-Flex-Cry1::EGFP together with (i) AAV-GFAP-mCherry::Cre, (ii) AAV-Syn-mCherry::Cre, or (iii) AAV-GFAP-EGFP, as a Cre negative control group (Fig. 2, A to C, and fig. S2A). We confirmed high specificity and efficiency of Cre-dependent expression of Cry1::EGFP by evaluating post hoc the histological colocalization of the Cry1::EGFP signal with GFAP-mCherry::Cre or Syn-mCherry::Cre, respectively (Fig. 2, D and E). We further confirmed that the GFAP-driven Cre recombinase

Division of Neurobiology, MRC Laboratory of Molecular Biology, Cambridge CB2 0QH, UK.
***Corresponding author. Email: m.brancaccio@imperial.ac.uk (M.B.); mha@mrc-lmb.cam.ac.uk (M.H.H.)** †Present address: Division of Brain Sciences, Department of Medicine, Imperial College London, London W12 0NN, UK.
‡Present address: SWC for Neural Circuits and Behaviour, London W1T 4JG, UK.

efficiently restricts expression of Cry1 to astrocytes by colocalizing the Cry1::EGFP signal with the astrocytic marker AldH1L1 (*3*, *4*) (fig. S2B). Locomotor activity of mice was recorded before and after surgery under constant dim red light (DD) to assess the intrinsic free-running circadian rhythmicity. Before surgery, Cry1/2-null mice did not show any consistent circadian rhythmicity in DD (DD1). However, after surgery (DD2), and in contrast to Cre-negative control mice, both AAV-GFAP-mCherry::Cre–treated and AAV-Syn- mCherry::Cre–treated mice showed sustained circadian patterns of locomotor behavior (Fig. 2F and fig. S2A). The periods of the induced rhythms were consistent with the molecular cycles of Per2::Luc observed in SCN explants being >26 hours and with the astrocytically driven rhythm being ~1 hour shorter than that of mice with neuronally expressed Cry1 (Figs. 2F and 1H). Furthermore, across animals the number of Cry1::EGFP^{+} neurons correlated positively with the behavioral period, whereas when Cry1 was expressed in SCN astrocytes there was a negative relationship (Fig. 2G), supporting the view that increasing numbers of targeted neurons and astrocytes can drive the locomotor rhythm to a period progressively closer to that of the corresponding cell-autonomous TTFLs. Nevertheless, the daily profiles of circadian behavior were equivalent whether neuronally or astrocytically controlled (Fig. 2H and fig. S2C). Thus, SCN astrocytes can specifically instruct new circadian behavior in an otherwise-arrhythmic mouse.

Given that astrocytes are not directly connected to motor centers, we hypothesized that they rely on recruiting the (TTFL-incompetent) SCN neuronal circuitry to engage behavioral output. To test for such indirect mechanisms, we imaged single cell– and circuit–level TTFL dynamics in Cry1/2-null SCN slices during the early phases of neuronal or astrocytic Cry1 expression (Fig. *3*). Neuronal expression of Cry1 immediately generated robust cellular Per2::Luc oscillations, consistent with a direct effect on the neuronal TTFL and similar to that observed after nonrestricted expression of Cry1 (*8*) (fig. S3). In contrast, although expression of Cry1 in astrocytes also initiated stable long period oscillations, it took >7 days to do so (movie S1 and Fig. 3, A and B). Analysis of individual Per2::Luc^{+} cells in the SCN revealed that Cry1 expression in astrocytes produced a progressive strengthening of Per2::Luc cellular rhythms, with periods initially differing by >16 hours and slowly converging to a single ~28.5-hour period (Fig. 3, C and D). This progressive effectiveness of astrocytes is consistent with an indirect engagement of the wider neuronal circuit.

To monitor neuronal activity directly, SCN slices expressing Cry1 only in astrocytes were supertransduced with AAVs encoding the synapsin-driven red genetically encoded calcium indicator RCaMP1h (Syn-RCaMP1h) (*3*). This revealed astrocytically driven circadian oscillations of neuronal $[Ca^{2+}]_i$ that were phase-advanced to Per2::Luc by ~6 circadian hours, as observed in wild-type SCN (Fig. 3, E to I, and movie S2). Circadian peaks of $[Ca^{2+}]_i$ and clock gene expression travel across the SCNs in a stereotypical spatio-temporal wave, with neurons in the dorsal SCN phase-leading the ventral ones in a pattern strictly dependent on the SCN circuit properties (*14*, *15*). To confirm that astrocytically restricted Cry1 expression also established appropriate spatio-temporal patterns of neuronal $[Ca^{2+}]_i$ across the SCN, we compared the calcium signal in wild-type SCN and SCN with

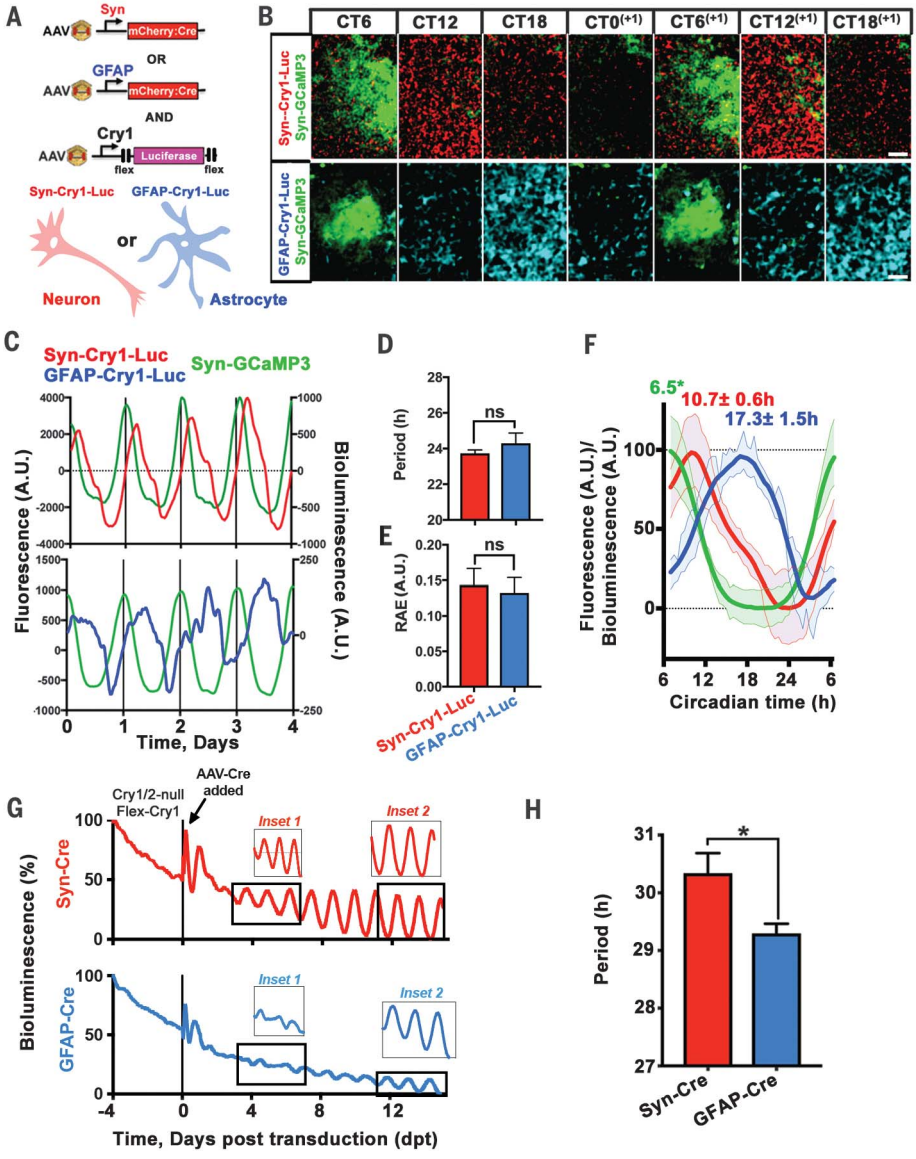

Fig. 1. An astrocytic clockwork can autonomously drive circadian clock gene expression in the SCN. (**A**) Experimental design to restrict expression of *Cry1*-Flex-Luc to neurons or astrocytes by AAVs cotransduced with Syn-mCherry::Cre or GFAP-mCherry::Cre. (**B**) Stills from live-image recordings of SCN slices cotransduced with *Cry1*-Flex-Luc, alongside Syn-mCherry::Cre or GFAP-mCherry::Cre, showing circadian variation of the bioluminescent *Cry1*-Luc signal, phase-aligned to Syn-GCaMP3. Signals are false lookup table colors. (**C**) Representative detrended traces of neuronally or astrocytically restricted *Cry1*-Flex-Luc circadian oscillations, phase-aligned to Syn-GCaMP3. A.U., arbitrary units. (**D** and **E**) Period and RAE values of *Cry1*-Luc oscillations, restricted to neurons or astrocytes. Data are means ± SEM, $n = 5$ per group. (**F**) Waveform traces of neuronal and astrocytic *Cry1*-Flex-Luc expression phase-aligned to Syn-GCaMP3. Data are means ± SEM, $n = 5$ for each experimental group. The asterisk indicates that the circadian phase is based on previous data (*3*, *9*). (**G**) Representative Per2::Luc traces from SCN slices of Cry1/2-null pups sequentially transduced with *Cry1*-Flex-Cry1::EGFP and then either Syn-mCherry::Cre or GFAP-mCherry::Cre AAVs to restore Cry1 expression in neurons or astrocytes, respectively. Insets show amplitudes of Per2::Luc in the early (inset 1) and late (inset 2) stages of neuronally and astrocytically restricted Cry1 expression. (**H**) Period values after neuronally or astrocytically restricted Cry1 expression in the late phases of the treatment. Data are means ± SEM, $n = 4$. Statistical test was an unpaired two-tailed t test. *$P < 0.05$. Scale bars, 50 μm.

astrocytically restricted Cry1 expression and found comparable dorsal-to-ventral organization of neuronal $[Ca^{2+}]_i$ (*16*) (Fig. 3, J and K, and movie S2). Given that *Per* gene promoters harbor calcium-responsive elements that phase-lock *Per* expression to neuronal $[Ca^{2+}]_i$, astrocytes may engage the E-box–based TTFL of neurons by driving neuronal $[Ca^{2+}]_i$ (*9*), sustaining intracellular oscillations of clock gene expression across SCN space and circadian time. Critically, this happens in the absence of *Cry* genes in neurons, thus revealing that the neuronal E-box–based TTFL may be dispensable for circuit-level circadian time-keeping. Thus, genetic complementation of Cry1 in SCN astrocytes can initiate and sustain mammalian circadian function by recruiting the latent SCN neuronal circuit.

To investigate the relevant mechanisms, we tested the role of connexin 43 (Cx43), a major component of gap junctions and hemichannels specifically expressed in astrocytes that coordinates astrocytic networks and was recently implicated in hypothalamic regulation of sleep-wake cycles (*17*, *18*). Cx43 is highly expressed in the SCN, extensively decorating astrocytic processes, as shown by colocalization with the GFAP-EGFP tag from control surgery mice (Figs. 2D and 4A). We then assessed the effects of Cx43 inhibition on circadian oscillations of clock gene expression in SCN slices by using the mimetic peptide TAT-Gap19 (*19*, *20*). TAT-Gap19 elicited a dose-dependent and reversible reduction in the amplitude and period lengthening of Per2::Luc oscillations (Fig. 4B and fig. S4), confirming the role of astrocytes in circadian function of wild-type SCN. We then showed that Cx43 inhibition by TAT-Gap19 significantly compromised Per2::Luc oscillations driven by astrocytically restricted expression of Cry1 in Cry1/2-null slices (Fig. 4, C and D). TAT-Gap19 specifically inhibits the hemichannel form of Cx43 that is involved in paracrine astrocytic release of gliotransmitters, including ATP and glutamate (*19*, *21*). Astrocyte-released glutamate is a major gliotransmitter in the SCN (*3*); therefore, we tested its key role in driving circadian rhythmicity in Cry1/2-null mice where Cry1 was expressed in astrocytes. Extracellular glutamate levels of Cry1/2-null SCN slices, measured using the AAV-encoded glutamate indicator iGluSnFR driven by Syn (*3*, *22*), exhibited no detectable circadian oscillations, but GFAP-Cre–restricted expression of Cry1 initiated robust circadian oscillations of glutamate. Moreover, these were strongly impaired by a Cx43 inhibitor (TAT-Gap19) (Fig. 4, E and F). These data support the role of astrocyte-derived circadian oscillations of glutamate in mediating astrocytic control of circadian oscillations in Cry1/2-null SCN.

To determine whether glutamate is specifically responsible for astrocyte-dependent circadian time-keeping in Cry1/2-null SCN, slices received DQP-1105, an antagonist for *N*-methyl-D-aspartate glutamate receptor assemblies containing the NR2C/D subunit (NMDAR2C) (*23*). NMDAR2C inhibition by DQP-1105 reversibly damps circadian rhythms of membrane potential and clock gene expression in wild-type SCN neurons (*3*).

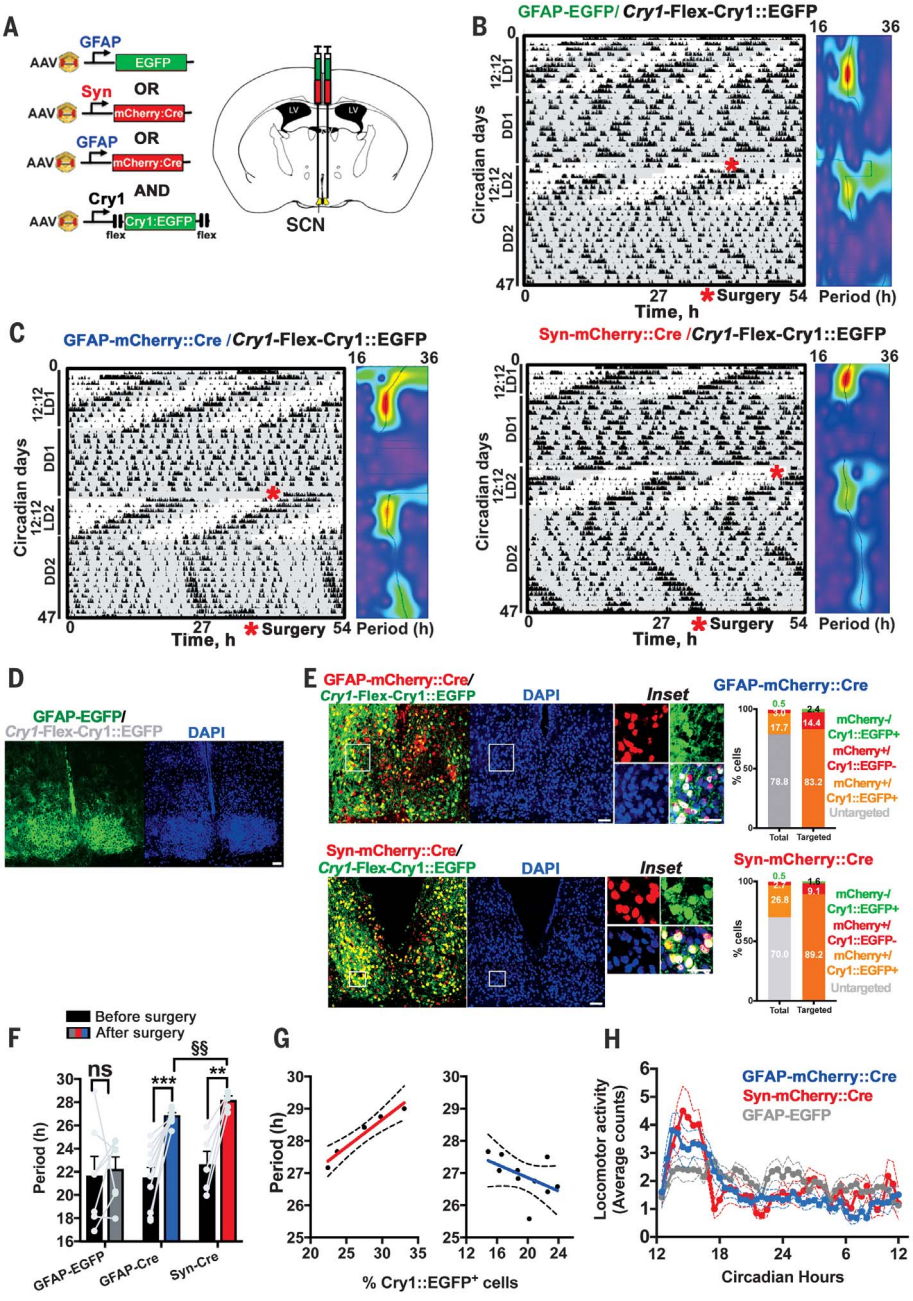

Fig. 2. Genetic complementation of Cry1 in SCN astrocytes initiates and sustains robust circadian patterns of locomotor activity in circadian-incompetent Cry1/2-null mice. (**A**) Experimental design of in vivo expression of Flex-Cry1::EGFP restricted to SCN astrocytes or neurons by Syn- or GFAP-driven Cre, respectively. (**B** and **C**) Representative actograms and wavelet analyses of Cry1/2-null mice targeted with *Cry1*-Flex-Cry1::EGFP together with AAVs expressing GFAP-EGFP (control) (B) or Cre (C). Rhythmicity in LD1 and -2 is due to a masking effect of the light-dark cycle. (**D** and **E**) Representative confocal tiled microphotographs of SCN sections from control and Cre-treated mice evaluated post hoc to assess effective targeting of the SCN. Histograms represent colocalization of fluorescence signals from mCherry::Cre and Cry1::EGFP in Cre-treated mice (insets). Total number of cells counted: GFAP-Cre, $N_{(DAPI^+)} = 5491$, $n = 5$ targeted mice; Syn-Cre, $N_{(DAPI^+)} = 6037$, $n = 5$ targeted mice. DAPI, 4′,6-diamidino-2-phenylindole. (**F**) Periods of circadian activity rhythms of control and Cre-treated mice before (DD1) and after (DD2) stereotaxic surgery. (**G**) Correlation analysis of number of Cry1::EGFP$^+$ astrocytes or neurons and behavioral period (Syn-mCherry-Cre: $r = 1$, $n = 5$, $P = 0.02$; GFAP-mCherry-Cre: $r = -0.70$, $n = 10$, $P = 0.03$, two-way Spearman test). (**H**) Locomotor activity plotted across the circadian day (means ± SEM). Group sizes were $n_{(GFAP\text{-}EGFP)} = 7$, $n_{(GFAP\text{-}Cre)} = 10$, and $n_{(Syn\text{-}Cre)} = 5$. The statistical test was a two-way repeated measures analysis of variance (RM-ANOVA) with Bonferroni correction. $^{**}P < 0.01$; $^{***}P < 0.001$; §§$P < 0.01$ (ad hoc unpaired two-tailed *t* test with Sidak-Bonferroni correction). Scale bars, 50 μm.

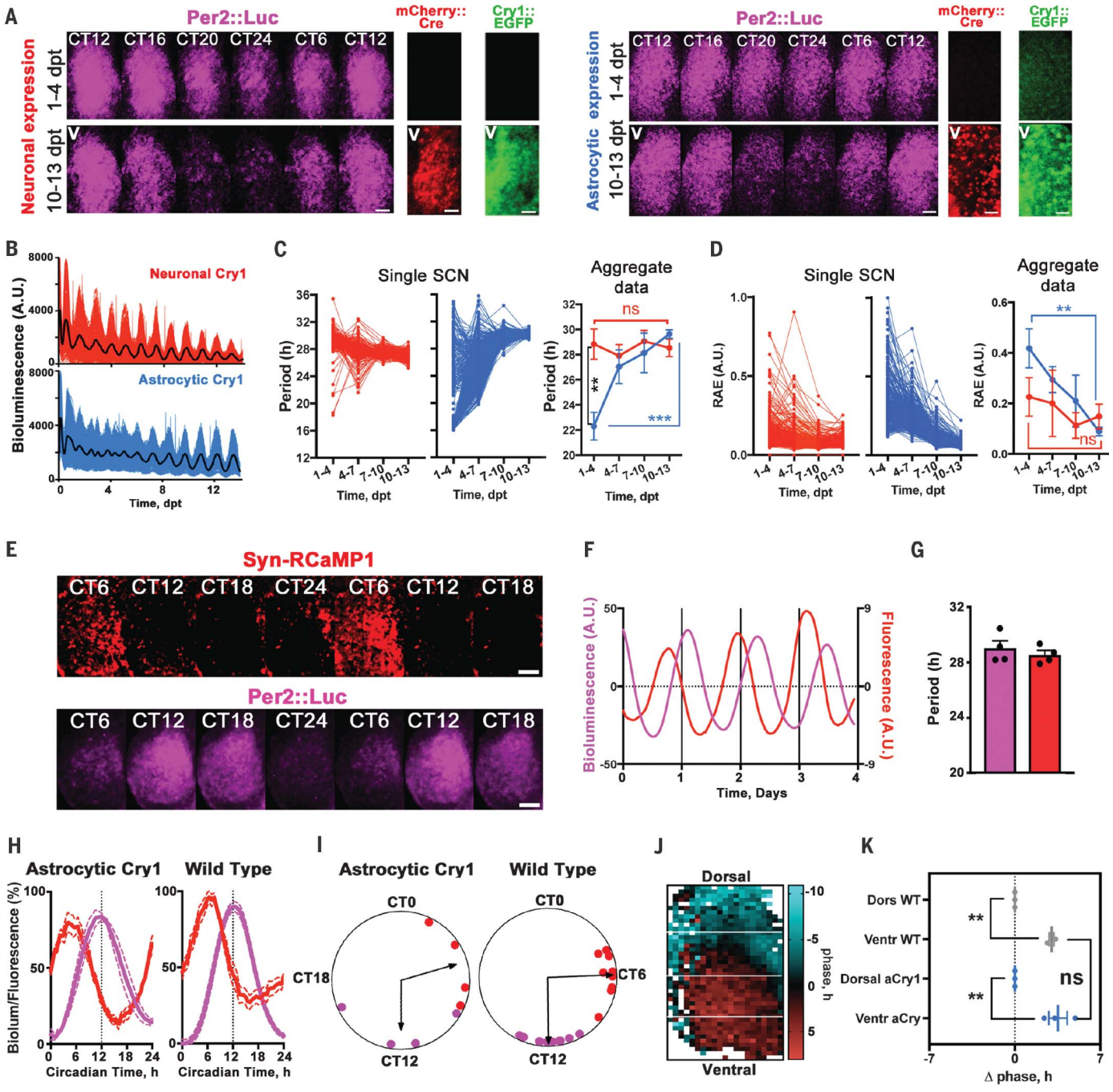

Fig. 3. Temporal dynamics of circadian bioluminescence rhythms of single cells initiated in Cry1/2-null SCN explants after neuronally or astrocytically restricted expression of Cry1. (**A**) Stills from live-image recordings of Per2::Luc expression from Cry1/2-null SCN slices, showing circadian variation of the bioluminescent signal in the early (upper rows) and late (lower rows) stages of neuronal or astrocytic Cry1 expression. Co-detected mCherry and EGFP are shown to compare spatial distribution and temporal dynamics of mCherry::Cre and Cry1::EGFP expression. (**B**) Representative single-cell (colored lines) and mean (black lines) traces of Per2::Luc oscillations after Cre-mediated expression of Cry1 in either neurons or astrocytes within SCN slices. (**C** and **D**) Period and RAE after neuronal or astrocytic expression of Cry1 in an individual SCN and across multiple explants. Traces for aggregate data are means ± SEM. Group size is $n = 3$ for each group. The statistical test was a two-way RM-ANOVA with Bonferroni correction. (**E**) Stills from live-image recordings showing circadian variations of Per2::Luc and Syn-RCaMP1h in Cry1/2-null SCN slices transduced with GFAP-mCherry::Cre or *Cry1*-Flex-Cry1::EGFP. (**F**) Representative traces of data presented in (E). (**G**) Period quantification of Per2::Luc and Syn-RCaMP1h in Cry1/2-null SCN expressing Cry1 only in astrocytes. Data are means ± SEM, $n = 4$. (**H** and **I**) Mean traces ± SEM (H) and Rayleigh plots (I) showing waveforms and phase differences of Per2::Luc and Syn-RCaMP1h oscillations in GFAP-mCherry::Cre or *Cry1*-Flex-Cry1::EGFP SCN slices and wild-type SCN. (**J** and **K**) Representative spatial phase map of Syn-RCaMP1h signal (J) and quantification of the dorsal-to-ventral phase relationship (K) in SCN expressing astrocytic Cry1 in comparison to wild type. Phase data were normalized to dorsal values. Values are means ± SEM, and group sizes are plotted. $^{**}P < 0.01$; $^{***}P < 0.001$; $^{****}P < 0.0001$. Statistical tests included a paired two-tailed *t* test (G) and unpaired ANOVA (K). Scale bars, 50 μm.

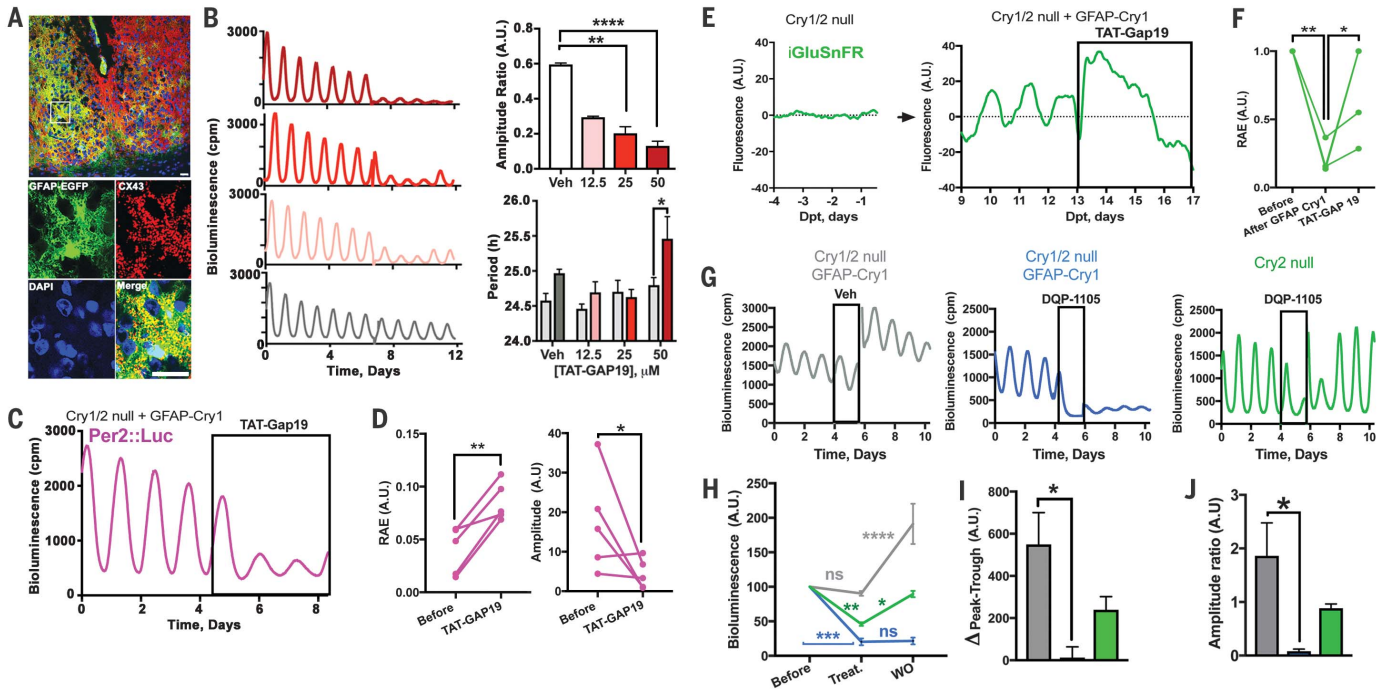

Fig. 4. Astrocytically released glutamate mediates astrocytic control of circuit-level circadian time-keeping in Cry1/2-null SCN expressing GFAP-restricted Cry1. (**A**) Confocal tiled microphotographs of adult SCN showing colocalization of GFAP-EGFP and Cx43, detected by polyclonal antiserum (results are representative of findings with three independent brains). (**B**) Representative Per2::Luc PMT traces and group data (mean + SEM), showing dose-response effects of TAT-Gap19 on the amplitude ratio (with drug/before drug) and period in wild-type SCN slices. The statistical test for the amplitude ratio was an unpaired ANOVA with Bonferroni correction. Analysis for period employed a two-way RM-ANOVA with Bonferroni correction [n = 3 for each group, except vehicle (Veh), n = 4]. (**C** and **D**) Representative Per2::Luc PMT trace (C) and paired scatter plot of RAE and amplitude (D) of Cry1/2-null SCN slices transduced with GFAP-mCherry::Cre and *Cry1*-Flex-Cry1::EGFP and treated with TAT-Gap19 (50 μM). The statistical test was a paired one-tailed t test, n = 5. (**E** and **F**) Representative iGluSnFR traces (E) and paired scatter plot of RAE (F) of Cry1/2-null SCN slices before and after GFAP-mCherry::Cre and *Cry1*-Flex-Cry1::EGFP transduction and treatment with TAT-Gap19 (50 μM). The statistical test was an RM-ANOVA with Bonferroni correction, n = 4. (**G**) Representative Per2::Luc PMT traces of Cry2-null and Cry1/2-null SCN slices transduced with GFAP-mCherry::Cre and *Cry1*-Flex-Cry1::EGFP and treated with DQP-1105 (50 μM) or vehicle, with subsequent washout. (**H**) Group data (means + SEM) of bioluminescence baseline traces represented in (G) before, in the presence of, and after removal of DQP-1105. The statistical test was a two-way RM-ANOVA with Bonferroni correction. (**I**) Group data (means + SEM) showing peak-trough differences in the presence of DQP-1105 of traces represented in (G). (**J**) Group data (means + SEM) showing amplitude ratio (after drug/with drug) of data presented in (G). The statistical test for (H) was a two-way RM-ANOVA with Bonferroni correction. The statistical test for (I) and (J) was an unpaired ANOVA with Bonferroni correction (n = 4 for Cry2-null and Veh groups; n = 3 for DQP-1105 treatment in Cry1/2-null group). $^*P < 0.05$; $^{**}P < 0.01$; $^{***}P < 0.001$; $^{****}P < 0.0001$ (n = 4). Scale bars, 20 μm.

The effect of the drug was much more marked in Cry1/2-null SCN with rhythms driven by astrocyte-expressed Cry1, as shown by the immediate drop in the baseline of the Per2::Luc rhythms and abolition of the peak-to-trough difference. Moreover, rhythmicity was restored upon washout of the drug, but the amplitude was irreversibly reduced. We interpreted this as protracted misalignment of circadian activity of SCN neurons and astrocytes. The pronounced effects of DQP-1105 were not evident in Cry2-null SCN, which retained Cry1 expression in both neurons and astrocytes, thus ruling out any confounding impact of Cry2 deficiency in our astrocytic Cry1 rescue model (Fig. 4, G to J). Thus, glutamate is a necessary mediator of astrocytic control of circadian function in the SCN, as shown by two independent pharmacological approaches: interference with glutamate release by astrocytes (via Cx43 inhibition) and with neuronal glutamate sensing (via NMDAR2C antagonism) (*2*, *3*).

A growing body of evidence has challenged a neurono-centric view of the control of behavior in mammals by showing that astrocytes can modulate complex neural processes, including cognition, fear, sleep, and circadian rhythms (*3*, *4*, *17*, *24*, *25*). However, most studies rely on the presence of a preexisting neuronally encoded behavior and show that behavioral performances are affected when astrocytic function is modified (*24*). Thus, regardless of the specificity of the astrocyte-neuron interactions described (*3*, *25*, *26*), those studies only addressed the ability of astrocytes to modulate neuronally dependent behavior; they did not establish their sufficiency in controlling behavior. Here, we have shown that astrocytes of the SCN can autonomously encode circadian information and instruct their neuronal partners, which lack a competent TTFL clock, to initiate and indefinitely sustain circadian patterns of neuronal activity and behavior.

REFERENCES AND NOTES

1. M. Koch, *Cell* **171**, 1246–1251 (2017).
2. M. H. Hastings, E. S. Maywood, M. Brancaccio, *Nat. Rev. Neurosci.* **19**, 453–469 (2018).
3. M. Brancaccio, A. P. Patton, J. E. Chesham, E. S. Maywood, M. H. Hastings, *Neuron* **93**, 1420–1435.e5 (2017).
4. C. F. Tso *et al.*, *Curr. Biol.* **27**, 1055–1061 (2017).
5. L. M. Prolo, J. S. Takahashi, E. D. Herzog, *J. Neurosci.* **25**, 404–408 (2005).
6. J. Livet *et al.*, *Nature* **450**, 56–62 (2007).
7. J. M. Fustin, J. S. O'Neill, M. H. Hastings, D. G. Hazlerigg, H. Dardente, *J. Biol. Rhythms* **24**, 16–24 (2009).
8. M. D. Edwards, M. Brancaccio, J. E. Chesham, E. S. Maywood, M. H. Hastings, *Proc. Natl. Acad. Sci. U.S.A.* **113**, 2732–2737 (2016).
9. M. Brancaccio, E. S. Maywood, J. E. Chesham, A. S. I. Loudon, M. H. Hastings, *Neuron* **78**, 714–728 (2013).
10. G. T. J. van der Horst *et al.*, *Nature* **398**, 627–630 (1999).
11. S.-H. Yoo *et al.*, *Proc. Natl. Acad. Sci. U.S.A.* **101**, 5339–5346 (2004).
12. M. R. Ralph, R. G. Foster, F. C. Davis, M. Menaker, *Science* **247**, 975–978 (1990).
13. V. M. King *et al.*, *Eur. J. Neurosci.* **17**, 822–832 (2003).
14. N. J. Smyllie, J. E. Chesham, R. Hamnett, E. S. Maywood, M. H. Hastings, *Proc. Natl. Acad. Sci. U.S.A.* **113**, 3657–3662 (2016).
15. M. Brancaccio *et al.*, *J. Neurosci.* **34**, 15192–15199 (2014).

16. R. Enoki *et al*., *Proc. Natl. Acad. Sci. U.S.A.* **114**, E2476–E2485 (2017).
17. J. Clasadonte, E. Scemes, Z. Wang, D. Boison, P. G. Haydon, *Neuron* **95**, 1365–1380.e5 (2017).
18. L. C. Mayorquin, A. V. Rodriguez, J.-J. Sutachan, S. L. Albarracín, *Front. Mol. Neurosci.* **11**, 118 (2018).
19. V. Abudara *et al*., *Front. Cell. Neurosci.* **8**, 306 (2014).
20. L. Walrave *et al*., *Glia* **66**, 1788–1804 (2018).
21. Z.-C. Ye, M. S. Wyeth, S. Baltan-Tekkok, B. R. Ransom, *J. Neurosci.* **23**, 3588–3596 (2003).
22. J. S. Marvin *et al*., *Nat. Methods* **10**, 162–170 (2013).
23. T. M. Acker *et al*., *Mol. Pharmacol.* **80**, 782–795 (2011).
24. J. F. Oliveira, V. M. Sardinha, S. Guerra-Gomes, A. Araque, N. Sousa, *Trends Neurosci.* **38**, 535–549 (2015).
25. T. Papouin, J. M. Dunphy, M. Tolman, K. T. Dineley, P. G. Haydon, *Neuron* **94**, 840–854.e7 (2017).
26. M. Martin-Fernandez *et al*., *Nat. Neurosci.* **20**, 1540–1548 (2017).

ACKNOWLEDGMENTS

We thank LMB Biological Services Group and the Ares staff for technical support. **Funding:** The Medical Research Council UK (core funding MC_U105170643 to M.H.H.) supported this work. **Author contributions:** M.B. designed, performed, and analyzed all experiments. M.H.H. contributed to the experimental design. M.D.E and N.J.S. developed and validated the *Cry1*-Flex-Luc and *Cry1*-Flex-Cry1::EGFP constructs. A.P.P, E.S.M., and J.E.C. conducted preliminary experiments. All authors contributed to project discussions. M.B. and M.H.H. wrote the manuscript. **Competing interests:** The authors declare no competing interests. **Data and materials availability:** All data are available in the manuscript or supplementary materials.

SUPPLEMENTARY MATERIALS

www.sciencemag.org/content/363/6423/187/suppl/DC1
Materials and Methods
Figs. S1 to S4
References (*27*, *28*)
Movies S1 and S2

23 February 2018; accepted 2 November 2018
10.1126/science.aat4104

Cell-autonomous clock of astrocytes drives circadian behavior in mammals

Marco Brancaccio, Mathew D. Edwards, Andrew P. Patton, Nicola J. Smyllie, Johanna E. Chesham, Elizabeth S. Maywood and Michael H. Hastings

Science **363** (6423), 187-192.
DOI: 10.1126/science.aat4104

Astrocytes can drive the master clock in the brain

The neurons of the suprachiasmatic nucleus (SCN) of the hypothalamus function as a central circadian clock, coordinating mammalian physiology with the 24-hour light-dark cycle. Brancaccio *et al.* found that these neurons have help from neighboring astrocytes (see the Perspective by Green). In mice lacking the *Cry* gene, which encodes a critical clock component, restoration of *Cry* expression and molecular clock function in the astrocytes, but not the neighboring neurons, restored rhythmic transcriptional oscillations in the SCN and reestablished circadian behaviors in the mice.

Science, this issue p. 187; see also p. 124